Protective action of saharian Anvillea radiata extracts against oxidative stress, inflammatory processes and diabetic neuropathy progression in high-fat-fed mice

Anne Mercier, Emilie Ricquebourg, Chouaib Kandouli, Marcel Culcasi, Sylvia Pietri

Protective action of saharian *Anvillea radiata* extracts against oxidative stress, inflammatory processes and diabetic neuropathy progression in high-fat-fed mice.

Anne Mercier [1], Emilie Ricquebourg[1], Chouaib Kandouli [1,2] Marcel Culcasi [1] and Sylvia Pietri [1,*]

[1] Aix-Marseille Univ, CNRS, ICR, UMR 7273, Molecular Probes in Biology and Oxidative Stress (SMBSO), Marseille, France; anne.mercier@univ-amu.fr; marcel.culcasi@univ-amu.fr; sylvia.pietri@univ-amu.fr
[2] Laboratoire de Biologie et Environnement, Faculté des Sciences de la Nature et de la Vie, Université des Frères Mentouri, Constantine, Algeria; chouaib50@gmail.com
* Correspondence: sylvia.pietri@univ-amu.fr (S.P.)

Received: date; Accepted: date; Published: date

Abstract: Diabetic neuropathies are of the major and earliest complications in diabetes and are associated with reactive oxygen species (ROS) production and inflammation in neurons and glial cells. We recently reported the antioxidant and antidiabetic properties of water-soluble extracts of the traditional medicine *Anvillea radiata* Coss & Dur (AR). The present study investigated whether AR aqueous and *n*-butanol polyphenol-enriched extracts could afford protection against diabetic neuropathy. In the i*n vitro* part of the study, antiglycative and ROS-producing enzymes inhibition capacities were demonstrated. In further experiments driven on AR-treated rat cell cultures, inflammation markers (TNFα, IL-6, IL-1 β) were measured in lipopolysaccharides-induced microglial cells and cytoprotection was evaluated on methylglyoxal-exposed astrocytes. In the in vivo part of the study, both extracts were given orally for 12 weeks at the dose of 75 mg/kg to high-fat-diet-C57BL/6J diabetic mice. Significant reduction of hyperglycemia and oxidative stress were observed, together with strong decrease of: i) thermal withdrawal latency (-30%) and T cells infiltration in sciatic nerve (-40%), ii) vasoconstriction, superoxide and protein carbonyls production in aortic rings, iii) myeloperoxidase and xanthine oxidase overactivation in plasma and kidney, iv) lipid peroxidation. Taken together, AR extracts may prove to be of therapeutic value in the management of diabetes complications.

Keywords: *Anvillea radiata*; traditional medicine; C57/BL6J mice; high fat diet; diabetic neuropathy; oxidative stress; inflammation; vascular damage; myeloperoxidase; advanced glycation end-products; microglial cells, astrocytes.

1. Introduction

Diabetes mellitus has become a major healthcare issue over the world and represents a panel of syndromes mainly characterized by chronic hyperglycemia and insulin disturbances. Among the main complications, diabetic neuropathies (DN), associating neuronal, glial and microvascular damage, are of the major and earliest ones in diabetic patients, taking complex and multiple forms [Duby 2004, Dewanjee 2018]. Hyperglycemia is susceptible to affect multiple metabolic routes associated to hallmarks including reactive carbonyl species such as methylglyoxal, advanced glycation end-products (AGEs)[Semba 2009, Vistoli 2013, Chaudhuri 2018], protein carbonyls (PCs) [Stocker 2015], and is also linked to changes in oxidative status and antioxidant pool [Yagihashi 2010, Dewanjee 2018]. Hyperglycemia-induced oxidative stress may cause an increase of myeloperoxidase (MPO) levels associated to endothelial dysfunction and related vascular and renal damages [Rovira-Llopis 2013; Galijasevic 2019]. Furthermore, the possible link between microglia activation, MPO expression and neuroinflammation as been reported [Jucaite 2015]. Diabetic neuropathies are linked to

mitochondrial dysfunction, increased production of reactive oxygen species (ROS), and a special focus has been done on their close relation with the inflammatory status, even at chronic subclinical grade [Zhou 2014]. Furthermore, even at pre-diabetic states, neurofunctional abnormalities have been reported in high-fat-fed (HFD)-mice in relation with the accumulation of ROS and other various species such as sorbitol and lipoxygenase, leading to unsaturated fatty acids oxidation and involved in endothelial dysfunction and inflammation [Obrosova 2007].

Complex mechanisms link hyperglycemia to neurodysfunction, presumably involving a cross-talk between oxidative stress and inflammation. The early prevention and treatment of hyperglycemia and its neurological consequences is therefore essential for the protection of the peripheral nervous system [Zhou 2014, Sandireddy 2014].

Even if diabetic neuropathies curative solutions are still to be developed, therapeutic strategies could rely on both pathogenetically-based and symptomatologic approaches [Dewanjee 2018, Pokhriyal 2018]. Pathogenesis-targeting therapies include - metabolic control by hypoglycemic agents and diet, - use of drugs active on DN ethiology with the aim to lower or prevent the oxidative stress and neurovascular damages. Among the best candidates are - benfotiamine that regulates both hexosamine and PKC pathways and increases glutathione (GSH) production [Hammes 2003], - antioxidants, radical scavengers or NADPH oxidase inhibitors to reduce oxidative stress, - aldose reductase inhibitors that lower sorbitol production by the polyol pathway [Varkonyi 2008, Dewanjee 2018], - inhibitors of AGEs formation or action, including polyphenols [Tang 2014, Khan 2020]. Benzoic acid hydrazides or thioxanthines belong to irreversible MPO inhibitors [Galijasevic 2019], but competitive MPO substrates such as flavonoids may also be active [Shiba 2008]. Symptomatic therapies aim to alleviate DN-induced pain and rely mainly on antidepressant, anticonvulsant or analgesic molecules [Varkonyi 2008].

Numerous studies have been devoted to the antidiabetic action of plant extracts and natural compounds but their impact on neurological complications has less often been investigated [Galuppo 2011, Singh 2013]. Phenolics known for their antioxidant activity can lower oxidative stress related to diabetic status, but they may also exert other beneficial effects against diabetes-induced neuropathies. A large panel of polyphenols such as resveratrol, phenolic acids and numerous flavonoids from natural origin were reported as AGEs inhibitors [Khan 2020]. Quercetin efficiently inhibits MPO activation [Shiba 2008, Loke 2008] and Gingko biloba extract (EGb761) exerts an anti-inflammatory action on microglial cells [Gargouri 2018]. Puerarin, an isoflavon glucoside used in traditional chinese medicine, improves nerve conduction velocity [Xie 2018] and the prescription BAIMEI-SAN was found to be efficient against peripheral neuropathy, improving nerve conduction and decreasing enzyme release and neurite loss in cortical cell cultures [Liu 2011]. Other medicinal extracts were reported to exert protection against diabetic neuropathies in diabetic rats by promoting myelination processes [Hao 2017] and improving sciatic nerve structural and functional features [Yang 2015].

We have recently investigated the antioxidant properties of polyphenol-enriched extracts of the Saharian traditional medicine *Anvillea radiata* Coss & Dur and showed that relevant biomarkers of type 2 diabetes and obesity were strongly improved by oral administration of these extracts in a model of HFD-fed mice [Kandouli 2017].

In the present work, we extended our focus area by investigating the properties of two water-soluble *Anvillea radiata* extracts in their protection against inflammation and diabetes-induced neuropathies. Afferent markers of diabetic neuropathies were studied *in vitro* including cellular models, and *in vivo* in HFD-fed mice, together with other biochemical and functional aspects characterizing diabetic renal and vascular complications

2. Materials and Methods

2.1. Standards, reagents and cell culture media

Buffers, reactants and enzymes, including glucose, hydrogen peroxide (H_2O_2), bovine serum albumin (BSA), xanthine oxidase (XO, from buttermilk), lipopolysaccharides from *Salmonella enterica* serotype typhimurium (LPS, ref L6143), L-phenylephrine hydrochloride, ACh perchlorate, diphenyleneiodonium (DPI), methylglyoxal, were purchased from Sigma Aldrich (Saint Quentin Fallavier, France). Purified myeloperoxidase (MPO, ref MY176) was supplied by Elastin Products Co (Owensville, USA) and 7-hydroxy-2-oxo-2H-chromene-8-carbaldehyde oxime (7-HCCO) was synthesized as previously reported [Stocker 2017]. HPLC grade solvents, including methanol, *n*-butanol and ethylacetate were from VWR Chemicals (Fontenay sous Bois, France). Media for cell cultures including CellTiter 96® Aqueous One Solution Cell Proliferation Assay kit (MTS) were purchased from Promega, France. CD3 antigen, Tissue-Tek O.C.T. Compound, anti-rabbit Alexa 555. Deionized water obtained from a Purelab station (Elga, France) was used throughout. Screening fluorescence assays were performed with a microplate spectrofluorimeter TECAN Infinite 200 (TECAN, Männedorf, Switzerland).

2.2. Plant material

The aerial parts of *Anvillea radiata* (flowers and leaves) were collected in the Algerian part of Sahara (El Oued, alt 69 m) in April 2013. The sample was identified by Prof. N. Khalfallah (Laboratoire de Génétique, Biochimie, et Biotechnologies Végétales, Université Frères Mentouri, Constantine, Algeria). A voucher specimen (LBE13/01) has been deposited in the herbarium of the Faculty of Natural and Life Sciences at Université des Frères Mentouri [Kandouli 2017]. Informations about the traditional use and preparation methods of the plant were obtained from local inhabitants.

2.3. Extraction of plant material

Extraction procedures leading to aqueous and organic extracts were driven as reported by Kandouli *et al*, 2017 [Kandouli 2017]. Preparation of *n*-butanolic extract (*n*-$BuOH_{extr}$): briefly, the dried plant material (200 g) was first extracted at room temperature for 24 h with methanol (1.2 L) then filtered and the procedure repeated twice. This extract was concentrated at 37°C until dryness under reduced pressure and treated with hot water (300 mL) to dissolve polyphenols, then filtered and the aqueous layer was successively extracted (4x100 mL) by petroleum ether (40-60°C fraction) to remove lipids, ethyl acetate and *n*-butanol to extract polyphenols. After reconcentration, 2.9g (1.4% w/w) of *n*-$BuOH_{extr}$ were obtained. Lyophilized aqueous extract (AQL_{extr}) was prepared from aqueous extraction of the dried plant material (10g) with hot water for 30 min. Filtration and lyophilisation at -80°C (Cryotec lyophiliser Cosmos, Saint-Gély-du-Fesc, France) afforded 15% w/w yield of AQL, which was stored at -20°C before use.

2.4. Inhibition of xanthine oxidase

Inhibiting effect of *A. radiata* extracts on xanthine oxidase (XO) was evaluated by microplate assay, measuring the inhibition of XO-catalyzed formation of uric acid from xanthine as previously reported [Kandouli 2017]. Briefly, 150 µL of sample solutions (18.5–600 µg/mL, final concentration) in phosphate buffer (PB, 200 mM, pH 7.5) were added in each well to 25 µL xanthine solution (50 µM, final concentration) and 25 µL EDTA solution (10 µM, final concentration) in PB (0.31% v/v DMSO). The reaction was started by addition of 50 µL of XO solution in PB (4.7 mU, final concentration) or buffer alone for control (CTRL). After 30 min incubation at 37 °C, absorbance was measured at 290 nm and inhibition of uric acid formation calculated as $((Abs_{CTRL} - Abs_{sample}) / Abs_{CTRL}) \times 100$, where Abs_{CTRL} and Abs_{sample} are respectively the net absorbance in absence or in presence of tested samples. Allopurinol and quercetin were used as standards.

2.5. Inhibition of myeloperoxidase

The activity of myeloperoxidase was evaluated as previously reported by Stocker *et al* [Stocker 2017] using 7-HCCO as a fluorescent probe for the detection of HOCl produced after adding H_2O_2.

Myeloperoxidase was added to 7-HCCO (150 µM) in 1X PBS (pH 6.5) in 96 wells microplate at 37°C in the absence (control, CTRL) or presence of extracts (XX mg/mL) or standards (XX µM), H_2O_2 (100 µM) was then added to start the reaction. The fluorescence was measured every 3 min (λ_{ex}=350 nm/ λ_{em}=470 nm); its variation (ΔF) was directly proportional to the amount of active MPO and a standard curve was used to determine the concentration of the hypochlorous acid produced. One unit (U) of the enzyme corresponds to the formation of 1 µmol HOCl per min at 37°C calculated from the initial rate of reaction with H_2O_2 as substrate. Inhibition of the specific MPO activity (As) was expressed as the ratio ($(As_{CTRL} - As_{sample}) / As_{CTRL}) \times 100$, where As_{CTRL} is the measured activity in absence and As_{sample} in presence of tested samples at a given concentration.

2.6. Inhibition of advanced glycated end-products (AGEs) formation in presence of BSA

BSA-Glucose assay: The procedure was driven as previously reported [Vidal 2014]. Briefly, BSA (50 mg/ml) was incubated with glucose (20 mM) in phosphate buffer (300 mM, pH 7.4) at 37 °C for 24h together with tested extracts or reference samples. Control was performed with BSA alone. Fluorescence of the advanced glycated end-products was monitored using a microplate spectrofluorimeter (λ_{ex}=330 nm / λ_{em}=394 nm). Half maximal inhibitory concentration (IC_{50}) values of AGEs inhibition were expressed as aminoguanidine equivalents.

BSA-methyglyoxal assay: The procedure was driven as previously reported [Vidal 2014]. Briefly, BSA (50 mg/ml) was incubated with glucose (20 mM) in phosphate buffer (300 mM, pH 7.4) at 37 °C for 24h together with tested extracts or reference samples. Control was performed with BSA alone. Fluorescence of the advanced glycated end-products was monitored using a microplate spectrofluorimeter (λ_{ex}=330 nm / λ_{em}=394 nm). Half maximal inhibitory concentration (IC_{50}) values of AGEs inhibition were expressed as aminoguanidine equivalents.

BSA-Formaldehyde assay: The procedure was adapted from a previous study [Mai 2020]. Briefly, BSA (XX mg/ml) was incubated with formaldehyde (10 mM) in phosphate buffer (300 mM, pH 7.4) at 37 °C for h together with tested extracts or standards. Control was performed with BSA alone. Fluorescence of the advanced glycated end-products was monitored using a microplate spectrofluorimeter (λ_{ex}= nm / λ_{em}= nm)

2.7. Experiments on rat neonatal microglial cells

Sprague-Dawley neonatal rat primary microglial cells were prepared according to the protocol of Ni *et al* [Ni 2010]. Experiments were adapted from procedures reported previously [Gargouri 2018]. MTT cell viability assay: microglial cells (3×10^5 cells/well) were plated on 96-well microplates and incubated for 24h in 10% CO_2 at 37°C with *A. radiata* extracts (10–20 µg/mL). After treatment, cells were incubated with MTS Assay kit (20 µl) for 4 h. After incubation for 24 h at 37 °C in an atmosphere of 5% CO_2, the supernatant was removed and the formazan crystals formed in the viable cells were solubilized in dimethylsulfoxide (DMSO). Absorbance was measured at 570 nm by using an ELISA MRX micro-plate reader (Dynex Technologies, Chantilly, USA). MTT (0.5 mg/ml) was added to the medium, incubation was extended for 1 h and the conversion of MTT to a purple formazan precipitate was monitored at 570 nm [Culcasi 2012]. *TNFα, IL-6, and IL-1 β release by microglial cells*: A LPS stock suspension was prepared in sterile phosphate-buffered saline (PBS, 5 mg/ml). Cultured primary microglial cells were pre-incubated with *A. radiata* extracts (XX µg/ml) for 30 min and then treated with or without (CTRL) LPS (10 ng/ml) for 24 h. Supernatants were then collected and centrifuged (1000 × g, 5 min, 4 °C). Release of TNFα (A), IL-6 (B) and IL-1β (C) were measured by ELISA assay (source??). PGE2 and 8-iso-PGF2α production were assessed in the supernatants with a commercially available enzyme immunoassay (EIA) kits (Biotrend, Cologne, Germany or Cayman Chemicals, Ann Arbor, Michigan, USA, respectively). For PGE2, standards from 39–2500 pg/ml were used and the lower limit of quantification (LLQ) of the assay was 36.2 pg/ml. The 8-iso-PGF2α assay has a range of standards from 0.5–500 pg/ml with a LLQ of approx. 3 pg/ml. Values are presented as the mean ± SEM of 4 independent experiments in triplicate. Statistical analyses were carried out by using one-way

ANOVA and Tukey posthoc test with *: $p < 0.05$ and ***: $p < 0.001$ against the LPS-stimulated positive control.

2.8. Activity of A. radiata extracts on MGO-exposed rat primary astrocytes

Primary astrocytes were isolated from 1 day Sprague-Dawley rats and treated according to the procedure reported by Chu *et al* [Chu 2014]. To assess the effect of MGO exposition and the activity of extracts, cells (3×10^5 cells/well) were seeded on 96 wells microplates in DMEM low glucose medium supplemented with 1% fetal bovine serum and MGO (700 μM) was added. Cells were then incubated for 24 h with extracts (XX mg/ml) or without. Astrocytes viability was estimated from an MTT assay (see paragraph 2.7) and compared to untreated cells.

2.9. Animal and study design

Standard diet (SD; 11% energy by fat) and high-fat diet (HFD, 60% energy by fat) were purchased from Safe (Augy, France). All diets contained 20% proteins. Animal care and experimental procedures were performed according to the rules of the European Union Council (Revised Directives 2010/63/EU). This protocol was subjected to the scrutinity of the local Animal Research Ethics Committee and was approved for the project FEDER-AdiabaOx (2008, N° 13851). Aix Marseille University and the CNRS have a license for animal housing and experimentation (agreement C13-055-06) and the study was under the supervision of a vet at the CNRS. Seventy-two 4 weeks-old female C57BL/6 J mice were purchased from CERJ (Janvier Labs, Le Genest St Isle, France) and maintained under conventional conditions with controlled temperature (22 ± 3 °C) and a 12 h light/ dark cycle and access to food and water ad libitum. An enriched environment, by using wheels, tunnels and toys, was given to promote physical and social activity. After one week acclimatization mice were assigned to the following experimental protocols: A first protocol examined the acute oral toxicity of AQL and *n*-butanol extracts at 2000 mg/kg on 16-weeks SD animals (n = 4/group) according to the procedure of Yamanaka *et al.* (1990). A second protocol consisted of a dose-response study of the acute hypoglycemic activity of the extracts on 16-weeks HFD animals in comparison with glibenclamide (n = 6/group) as detailed below. Based on our previous results on AQL and *n*-BuOH extracts toxicity (non toxic up to 2000 mg/kg) and acute hypoglycemic activity by oral administration on C57BL/6 J mice [Kandouli 2017], the dose of 75 mg/kg per day was retained for the present work. Mice (n = 72) were randomly divided into 6 experimental groups (n = 12): controls (given SD for 28 weeks); HFD group (given HFD for 28 weeks); [HFD+AQL_{75}] group, given HFD for 16 weeks, followed by HFD supplemented with AQL (75 mg/kg) for 12 weeks; [HFD+*n*-$BuOH_{75}$] group, given HFD for 16 weeks, followed by HDF supplemented with butanol extract (75 mg/kg) for 12 weeks; [HFD+Met_{150}] group, given HFD for 16 weeks, followed by HFD supplemented with metformin (150 mg/kg) for 12 weeks and [HFD+Met_{75}+AQL_{75}] group, given HFD for 16 weeks, followed by HFD supplemented with a mixture of metformin and AQL_{extr} (both at 75 mg/kg) for 12 weeks. Weekly weights measurements and daily estimates of food intake and clinical signs of suffering, weight loss and moribundity were recorded. At weeks 16 (before incorporation of extracts in the food) and 28, blood samples were collected from tail vein under local anaesthesia induced by 0.25% lidocaine application in ointment. Blood glucose concentration was measured using a commercial whole-blood glucose auto analyzer (Freestyle Optium Neo, Abbott)

2.10. Glucose and insulin plasma levels and lipid metabolism

2.11. Plantar Test

The thermal withdrawal latency was measured according to the protocol described by De Gregorio *et al* [De Gregorio 2018]. In a room kept at 25°C, mice were placed in an acrylic box provided with an infrared (IR) light (UgoBasile Plantar Test, Varese, Italy) 20 min before experiment. The IR light (40% of power) was placed beneath of the mid-plantar surface of hind paws and the withdrawal responses were automatically recorded, with a cut-off latency of 15 s to prevent hind paw damage.

The stimulation was repeated three times with an interval of 5 min and repeated three consecutive days. Data were expressed as the mean of withdrawal latency registered each day.

2.12. T cells infiltration in the sciatic nerve

T cells infiltration in the sciatic nerve was measured following the procedure of De Gregorio *et al* [De Gregorio 2018]. Sciatic nerves were carefully excised at week 33 from diabetic and control mice, fixed in phosphate buffer (XX mM, pH, 4% paraformaldehyde) for 24 h at 4°C and then kept in sucrose (30%) for 24-72 h at 4°C and embedded in Tissue-Tek O.C.T. Compound. Longitudinal thick nerve cryosections were placed on silanized slides. The samples were then blocked for one hour in 5% fetal bovine serum, 0.025 Triton X-100, 0.5 M Tris buffer (pH) and incubated overnight with anti-mouse CD3 (Dako, Santa Clara, USA, 1:100). They were then washed three times with 0.025 Triton X-100, 0.5 M Tris buffer and incubated (25°C, 2h) with secondary antibody (1:300, anti-rabbit Alexa 555, Cell Signa Technology, Danvers, USA). The number of CD3+ cells was quantified and normalized versus nerve area.

2.13. Isolated aortic rings preparation and treatments

Protocols driven for the preparation and treatment of aortic rings were as previously reported by Cassien *et al* [Cassien 2016]. At week 33, mice were deeply anesthetized by intraperitoneal injection of sodium pentobarbital (100 mg/kg; Ceva Santé Animale, Libourne, France) before thoracotomy. The aortas were removed, cleaned and cut into 3-mm ring segments, mounted between two stainless steel hooks and suspended at 37 °C in oxygenated, isolated 10 mL baths filled with a modified Krebs-Henseleit (KH) buffer (pH 7.35) containing (in mM): NaCl, 118; KCl, 4.7; KH_2PO_4, 1.5; $CaCl_2$, 2.5; $MgSO_4$, 1.2; $NaHCO_3$, 25; EDTA, 0.5; glucose, 11. The medium was renewed every 20 min and continuously aerated with a 5% CO_2-95% O_2 gas mixture. Changes in tension were recorded using a standard apparatus (Harvard Apparatus, Les Ulis, France). Rings were first equilibrated for 60 min at 1 g of resting tension and then stretched step by step until optimal and reproducible reference contraction to high-potassium physiological salt solution (KPSS, 123 mM KCl) was obtained. Then, after a 20 min wash out, rings were contracted to 50% of the KPSS response by 10-7 M L-phenylephrine hydrochloride and endothelial integrity was tested by adding 10^{-5} M ACh perchlorate (ou Cl-IBEMECA, cf Nishat 2016) to the medium. The endothelium was considered intact if ACh induced a relaxation of 80% or higher and the rings fulfilling this condition were reequilibrated for 30 min in KH buffer before the experiments.

We also examined the protection afforded by *A. radiata* extracts against tissue damage caused by endogenous $O_2^{-\bullet}$ release as a result of NADPH stimulation of endothelial NADPH oxidase. Rings were first preincubated for 30 min in KH buffer containing 0.1% DMSO containing the selected extracts (10 mg/ml) and 30 μM DTC (Sigma-Aldrich), then NADPH (1 mM) was added and incubation was prolonged up to 60 min. Two equal sets of individual rings were then transferred into separate wells prefilled with 0.3 mL of the same KH buffer/extracts or vehicle/NADPH mixture as described above, and further incubated for 30 min in the dark at 37°C. One subset of rings was kept for tissue protein carbonyls measurements and the other subset was used for EPR experiments. Briefly, to each well containing NADPH-stimulated rings in KH buffer was added an aliquot of the selected extracts in DMSO as to reach a final concentration of 15 mM PBN and 1% DMSO, and the mixture was incubated for 20 additional min. For each extract, three 300 mL-aliquot of the mixture were placed in 1 mL *Nalgene® cryogenic vials* and immediately stored in liquid nitrogen for delayed EPR analysis. Control wells were performed without NADPH. In additional experiments, NADPH oxidase was inhibited by adding DPI (15 mM) to the medium during the 30 min preincubation phase.

2.14 EPR analysis of PBN spin trapping in aortic rings

Previously frozen samples of aortic rings(see above) were thawed just prior to use, placed into capillary glass tubes and EPR spectra were recorded 45 sec after sample thawing, on a Bruker ESP 300

spectrometer (Karlsruhe, Germany) with the following instrument settings: modulation frequency 100KHz, microwave power 10 mW, field axis resolution 2048 pts, modulation amplitude 0.07 mT, time constant 81.92 ms, receiver gain 8 x 10^4, scan rate 0.31 mT/s, sweep width, 13 mT, 10 accumulated scans.

2.15. Protein carbonyls determination in aortic tissue

Protein carbonyls content was evaluated in ring tissues homogenates according to the protocol of Stocker *et al* [Stocker 2015] using the 7-hydrazino-4-nitrobenzo-2,1,3-oxadiazole (NBDH, Sigma-Aldrich) as a probe to form highly fluorescent derivatives with aldehydes via hydrazone formation. Homogenates were prepared by homogenizing 0.1 g of fresh aortic tissue powdered in liquid N_2 in 1.15% KCl ice-cold solution. After centrifugation (3000×g, 40 min, 2–3 °C), supernatants were diluted 10-fold with PBS 0.1 X. Protein concentrations were determined using the BCA protein assay kit (Thermo Fisher Scientific). Then 100 µL of diluted samples were placed in 96-well microplates and reacted for 15 min at room temperature with an aliquot (100 µL) of the NBDH assay kit (Carbofax®; Yelen) and concentrations in NBDH-reacted carbonyls were determined by fluorimetry (TECAN Infinite 200, λ_{exc} = 500 nm, λ_{em} = 560 nm) relative to standard calibration curves built from oxidized BSA. The protein carbonyl content was expressed as nanomoles/mg protein.

2.16. Myeloperoxidase activity in mice plasma

MPO activity was evaluated as previously reported in Stocker *et al* [Stocker 2017] using 7-HCCO as a fluorescent probe for HOCl detection. Plasma were collected from control and diabetic mice at week 33, then diluted ten-fold in 1X PBS pH 6.5. Ten µl of 7-HCCO (100 µM, final concentration) and five µl H_2O_2 (100 µM, final concentration?) were added to 150 µl of diluted plasma and the fluorescence recorded each 3 min (λ_{ex} = 350 nm, λ_{em} = 470 nm). Active MPO content was estimated from the relative fluorescence using a calibration curve built with purified human MPO in plasma.

2.17. MDA-TBA assay in mice plasma

Lipid peroxidation was evaluated through malondialdehyde-thiobarbituric acid (MDA-TBA) formation assay [Stocker 2017]: Aliquots (50 µL) of plasma were added in test tubes to a mixture of 450 µL of thiobarbituric acid solution in orthophosphoric acid (0.3 M, pH 3.5) and 10 µL of butylated hydroxytoluene solution (5 mM) in ethanol. Samples were heated at 95 °C for 30 min, then cooled back to room temperature and centrifuged (1800 × g, 10 min). The supernatant content in MDA-TBA adduct was assayed by HPLC (Merck Hitachi/Lachrom HPLC system: autosampler, pump L-7100, fluorescence detector L-7480, interface D-7000, degasser L-7612, with Agilent EZChrom Elite Compact software (Pleasanton, USA)). Analyses were performed using a C18-bonded Macherey-Nagel silica column (250 mm × 4.6 mm, 5 mm) and fluorescence detection (λ_{ex} = 532 nm, λ_{em} = 553 nm). Samples (20 µL) underwent isocratic elution (A/B: 50/50), solvent A: 20 mM phosphate buffer (pH 6.9) and solvent B: methanol, at a flow rate of 1 ml/min for 10 min, with peak area quantification. MDA-TBA levels were calculated from a standard curve of MDA tetrabutylammonium and are the means of three independent experiments in each group made in triplicate. Data are expressed in nmole/mg protein.

2.18. Evaluation of myeloperoxidase and xanthine oxidase activities in kidney homogenates

Kidney sample were collected at week 33, washed with PBS 1X, then homogenized in RIPA buffer and centrifuged (12,000 rpm, 10 min) at 4°C and stored at -80°C as reported by Chowdury *et al* [Chowdury 2019]. MPO activity was measured as reported in paragraph 2.6. Evaluation of XO activity was performed by microplate assay by adding in each well 10 µl of tissue homogenate, 190 µl of phosphate buffer (50 mM, pH 7.5) and 100 µL of xanthine solution in PB (75 µM, final concentration). After incubation at XX°C for XX min, absorbance was measured at 290 nm and XO activity calculated as reported in paragraph 2.4.

3. Results and Discussion

3.1. Anvillea radiata aerial parts extraction processes and phenolic content characterization

Extraction of the aerial parts of the plant *A. radiata* and HPLC analysis of their phenolic content were driven as reported in Kandouli *et al* [Kandouli]. Petroleum ether extraction allowed the removing of lipids from the initial methanolic extract, which was reconcentred and taken back with hot water. Then further successive extractions of the resulting aqueous layer with ethyl acetate and *n*-butanol (*n*-BuOH) allowed to separate less ($EtOAc_{extr}$) and more ($n\text{-}BuOH_{extr}$) polar fractions (Fig.1). In our previous study on *A. radiata* extracts anti-diabetic properties, phenolic profile analyses indicated that the main organic (MeOH, EtOAc, n-BuOH) and aqueous (AQL) extracts were rich in flavonoids (~41-57%) and hydroxycinnamic acid derivatives (~40-58%), while rather poor in hydroxybenzoic acids (~2-4%). Furthermore, administration of extracts to HFD-fed mice has resulted in a significant decay of hyperglycemia and in a regulation of the lipid profile, together with a lowering of inflammation markers [Kandouli 2017]. In the present study, HPLC analysis led to similar results (data not shown) and we selected two of these extracts, the aqueous lyophilized (AQL_{extr}) and the *n*-butanolic one ($n\text{-}BuOH_{extr}$) from their phenolic profile, (flavonoids, mg RUE/g DW: AQL_{extr} 14.4 ± 0.8, $n\text{-}BuOH_{extr}$ 33.3 ± 1.9; hydroxycinnamics, mg CAE/g DW: AQL_{extr} 17.1 ± 1.3, $n\text{-}BuOH_{extr}$ 51.7 ± 4.0; hydroxybenzoics, mg GAE/g DW: AQL_{extr} 1.5 ± 0.0, $n\text{-}BuOH_{extr}$ 3.8 ± 0.2), their antioxidant and digestive enzyme inhibition capacities, together with their low cytotoxicity and good solubility. These extracts have also been shown to improve metabolic parameters, reduce hyperglycemia and dyslipidemia on HFD-fed mice [Kandouli 2017].

The Asteraceae family was reported to be of potential interest in the management of diabetic complications, due to the high content in flavonoids, polyphenols, terpenoids, saponins, polysaccharides and alkaloids [Singh 2013]. Flavonoids such as breviscapin from *Erigon breviscapus* and silibinin from *Silybum marianum* were found to protect respectively against cardiac dysfunctions, myocardial Ca^{2+} impairment and nephropathy in streptozotocin-induced diabetic rats [Singh 2013]. *Anvillea radiata* belongs to this Asteraceae family and is known for its traditional use against diabetes mellitus in Algerian Sahara. However, to our knowledge, its properties against diabetes related neuropathies have still not been investigated.

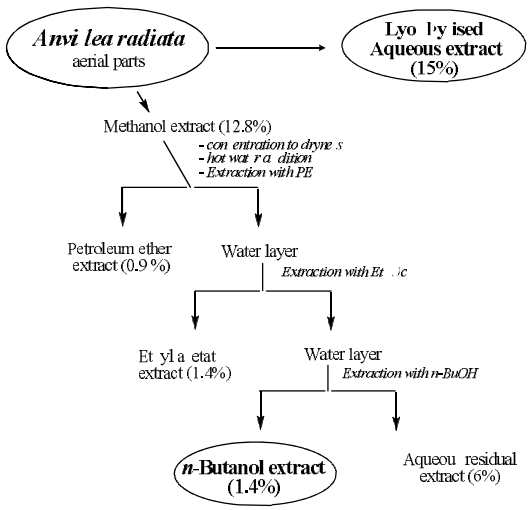

Figure 1. Preparation of *Anvillea radiata* aqueous and organic extracts.

3.2. In vitro evaluation of xanthine oxidase and myeloperoxidase inhibition and anti-glycative effect (BSA-glucose, BAS-methyglyoxal and BSA-formaldehyde systems) of extracts

3.6 Thermal withdrawal latency

A plantar sensitivity test was used to assess the symptomatic progression of diabetic neuropathy in HFD-fed mice and to measure the protection provided by *A. radiata* extracts. The paw withdrawal latency triggered by a thermal stimulation allowed us to evaluate the peripheral nerve functional loss/protection. The assay was repeated from week 5 to week 33, starting the administration of each extracts (75 mg/kg) at week 21. Diabetes-induced hypoalgesia, as observed from the strong latency increase observed for HFD- compared to SD- fed mice at week 33, was lowered by about 30% when extracts were given, which demonstrates their efficiency even after long term T2DM induction. If short term diabetes may induce hyperalgesia, long term exposition was reported to induce merely hypoalgesia [Uddin 2020]. *A. radiata* polyphenolic extracts are characterized by a high representation of flavonoids and hydroxycinnamic acids. Flavonoids, depending of their structure, are susceptible to interact through many DN-related processes from reduction of oxidative stress, increased levels of antioxidant enzymes SOD, CAT, GPx (catechin, naringenin, kaemperol, luteolin, rutin, genistein…), to reduction of MDA (catechin, luteolin, rutin, genistein…) and AGEs formation (kaempferol) or lowering of proinflammatory cytokine levels (TNFα, IL-1β, IL-6…). Behavioral markers may also be improved by flavonoids as for example thermal hypoalgesia which was reduced by baicalein treatment of STZ-diabetic mice [Basu 2020]. Various phenolic acids possess antioxidant and antidiabetic activities. Gallic acid administered to STZ-induced rats improved insulin secretion, lipid profile and others metabolic parameters [Latha 2011]. In the hydroxycinnamic series, ferulic acid was beneficial against diabetic neuropathy in STZ-rats by lowering both metabolic and neurologic alterations, improving the antioxidative status and reducing inflammation and apoptosis; combination with insulin enhanced the obtained protection [Dhaliwal 2020]. Zhang *et al* reported that chlorogenic acid (CA), an abundant food polyphenol, decreases voltage-gated potassium channels which are key regulators of membrane potential in sensory neurons, then decreasing neuronal excitability in neuropathic pain [Zhang 2014]. CA also protects neuronal cells under MGO induced apoptosis [Huang 2008]. The rosmarinic acid, an ester of caffeic acid, was shown to exert an anti-allodynic effect in STZ-induced diabetic rats [Hasanein 2014].

A **B**

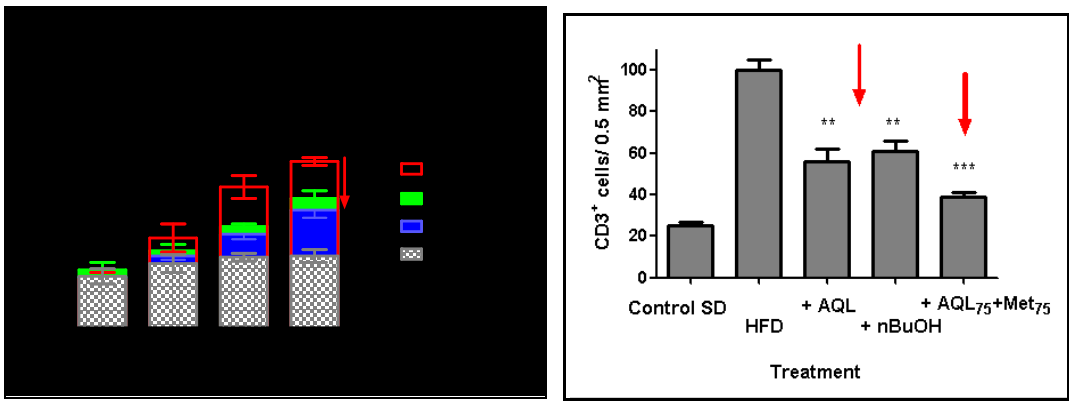

Figure 3: A/ Plantar test: measurement of the paw withdrawal latency (week 33) of treated C57BJ/6 HFD-fed mice compared to SD and HFD controls. **B/** T Cell infiltration (week 33) in sciatic nerve of C57BJ/6 HFD-fed mice. Both AQL and nBuOH extract were given at 75 mg/kg body weight.

3. 7 T cell infiltration in sciatic nerve

In addition to hyperglycemia-induced processes, obesity-associated low-grade chronic inflammation may also occur through adipose tissue dysfunctions and subsequent overexpression of pro-inflammatory factors such as TNFα from adipose or neural tissues, which may then elicit the recruitment of immune cells such as macrophages and T cells within the endoneurial area [Kosacka 2019]. We analyzed the infiltration of CD3 positive cells in the mice sciatic nerve as an inflammation marker in the peripheral nervous system. Sciatic nerves were carefully excised at week 33 from

diabetic and control mice and an immunofluorescence assay was performed against the CD3 antigen (Fig. 3B). The high infiltration level observed for the HFD group as compared to the SD group was lowered by about 40 % when HFD-fed mice were treated by extracts at the dose of 75 mg/kg. Of importance is the best result obtained by treatment with combined half doses of AQL+ Metformin (75 mg/kg each), while meftformin alone… In literature, caffeic acid phenyl ester (CAPE), a widespread phytoconstituent, exhibiting a large range of properties including antioxidant, anti-inflammatory and immunomodulatory activities was shown to protect the sciatic nerve of STZ-induced diabetic rats, reducing the total antioxidant status together with MDA and NO levels [Yucel 2012].

3.8. Vasorelaxant properties of extracts on isolated mice aortic rings

The peripheral nervous system is rather poorly microvascularized at the endoneurial level and furthermore the length of its axons makes them insufficient to insure by themselves trophic and other molecules transport to distal extremities. Such characteristics may contribute to increase the susceptibility of distal parts of the PNS towards diabetes-induced troubles. DN are associated to vascular damages at both macro and micro vascular levels, where structural changes may occur with in particular a thickening of the basement membranes and a narrowing of the vascular lumina with possible ischemia. Oxidative stress and MPO activation are known to be involved in vascular endothelium damages, leading to disturbances in vascular tone and enhanced vasoconstriction. We evaluated here the endothelium protection afforded by *A. radiata* extracts on HFD-fed mice aortic rings precontracted by the α1-adrenoreceptor agonist phenylephrine (PE) (Fig 4). Vasoconstriction was measured in response to the agonist. The best vasorelaxant effect was observed for AQL extract, giving quite 30 % protection compared to untreated HFD group. MPO is known to play an important inflammatory role in diabetes and exerts a vasoconstrictive action by NO consuming [Neogi 2012]. Actually, a positive correlation between MPO inhibition and vasorelaxation can be observed… for extracts.

3.9. Vascular protection against NADPH-induced superoxide in mice aortic rings

Addition of excess NADPH to the aortic rings incubation medium resulted in NADPH oxidase activation and superoxide production. We then evaluated the protection afforded by *A. radiata* extracts by spin trapping experiments and protein carbonyl measurements.

PBN spin trapping of NADPH-induced superoxide radical in aortic rings resulted in observation by EPR of PBN-OH spin adducts, derived from superoxide scavenging (Fig 5A). Extracts afforded…Superoxide quenching properties….

Protein carbonyl content: The activation of NADPH oxidase led to a strong increase of protein carbonyl content, which was considerably lowered in …groups, this result being in good accordance (Fig 5B) with the antioxidant and superoxide quenching properties of *A. radiata* extracts [Kandouli 2017].

3.10 MPO inhibition and protection against lipid peroxidation in plasma

MPO activity has been reported to induce NO consumption and vascular endothelial dysfunctions. Nishat *et al* highlighted the link between MPO level enhancement and the overexpression of the adenosine A3 receptor, involved in vasoconstriction processes [Nishat 2014]. Figure XX shows that plasmatic MPO levels where significantly enhanced in HFD-fed mice compared to SD group, while groups treated with extracts exhibited XX% reduction compared to HFD untreated mice, giving then the same trend than vasorelaxation results as shown in fig. XX.

3.11 Inhibition of XO and MPO in mice kidney homogenates.

The activity of XO in kidney homogenates was strongly increased in HFD-fed group compared to control mice. Treatment with both AQL and *n*-BuOH extracts considerably lowered this overactivation as shown in Fig. 6A. Moreover, administration of combined [AQL_{75} + MET_{75}] afforded the best protection, while metformin alone…. The same trend was observed for the detection of MPO

activation (Fig 6 B), with a ….. In diabetic renal disease, ROS overproduction may arise from various sources including XO, NADPH oxidase, mitochondrial electron-transport chain or MPO [Fakhruddin 2017]. XO has been shown to promote vascular inflammation and of the known inhibitors of the enzyme, febuxostat was reported to exert a protection against diabetic nephropathy in mice, to attenuate oxidative stress in blood vessels and to lower IL-6 and IL-1β inflammatory cytokine levels, while allopurinol protected human macrophages from ROS induced degradation linked to atherosclerosis [Mizuno 2019]. Then, the protection afforded through XO inhibition on diabetic mice may then occur merely by reducing inflammatory processes rather than lowering hyperuricemia or hyperglycemia as reported on obese KK-Ay mice with diabetic nephropathy [Mizuno 2019]. However, urate production through XO activity may in turn activate MPO and thereby lead to subsequent impairments [Neogi 2012].

4. Conclusions

Diabetic neuropathies represent a complex panel of multifactorial pathologies. Many therapeutic agents have been proposed to address the different pathways involved in DN progression, such as anti-glycative agents, aldose reductase inhibitors, anti-inflammatory and antioxidant molecules [Dewanjee 2018], but at the present time, there is still a need of safe and multitarget therapies. Phytochemical resources are good candidates for such approaches, owing to their rich composition in phenolics and flavonoids and the traditional knowledge associated with their use. Here we showed through administration of water-soluble AQL and *n*-BuOH extracts to HFD-fed mice that *A. radiata*, which is active in metabolic protection against T2DM may also afford a protection against DN, one of its main complications, being efficient on multiple DN-linked pathways. These extracts were shown to reduce oxidative stress and inflammation processes related to glycemic and lipidic dysregulations. They efficiently prevent AGEs and PC accumulation, reduce ROS formation by lowering the activity of enzymes such as XO and MPO, prevent ROS-induced damages through their antioxidant activity [Kandouli 2017], and enhance the antioxidant status, particularly by preventing GSH decay. As a result, even after long term T2DM induction on HFD-fed mice, we observed in mice treated by AQL and *n*-BuOH *A. radiata* extracts a vascular protection and an improvement of the peripheral nerve response, together with a reduction of its inflammation.

References

1. Duby, J.J; Campbell, R. K.; Setter, S.M.; White, J. R.; and Rasmussen, K. A. Diabetic neuropathy: an intensive review. *Am. J. Health-Syst. Pharm*. **2004**, *61*, 160-173. DOI: 10.1093/ajhp/61.2.160
2. Dewanjee, S.; Das, S.; Das, A. K.; Bhattacharjee, N.; Dihinghia, A.; Dua, T. K.; Kalita, J. ; Prasenjit, M. Molecular mechanism of diabetic neuropathy and its pharmacotherapeutic targets. *Eur. J. Pharmacol*. **2018**, *833*, 472-523. DOI: 10.1016/j.ejphar.2018.06.034
3. Yagihashi, S.; Mikusami, H.; Sugimoto, K. Mechanism of diabetic neuropathy: Where are we now and where to go? *J. Diabetes Invest*. **2011,** *2*, 18-32. DOI: 10.1111/j.2040-1124.2010.00070.x
4. *Semba, R.; Najjar, S.; Sun, K.; Lakatta, E.; Ferrucci, L.* Serum carboxymethyl-lysine, an advanced glycation end product, is associated with increased aortic pulse wave velocity in adults. *Am. J. Hypertens.* ***2009****, 22, 74–79.* doi: 10.1038/ajh.2008.320
5. Vistoli, G.; De Maddis, D. ; Cipak, A. ; Zarkovic, N. ; Carini, M. & Aldini, G. Advanced glycoxidation and lipoxidation end products (AGEs and ALEs): an overview of their mechanisms of formation, *Free Radic. Res.* **2013**, *47*:sup1, 3-27. DOI: 10.3109/10715762.2013.815348
6. *Chaudhuri, J.; Bains, Y.; Guha, S.; Kahn, A.; Hall, D.; Bose, N.; Gugliucci, A.; Kapahi, P.* The role of advanced glycation end products in aging and metabolic diseases: bridging association and causality. *Cell Metabolism.* ***2018****, 28, 337–352.* DOI: 10.1016/j.cmet.2018.08.014
7. Stocker, P.; Ricquebourg, E.; Vidal, N.; Villard, C.; Lafitte, D.; Sellami,L. and Pietri, S. Fluorimetric screening assay for protein carbonyl evaluation in biological samples. *Anal Biochem*. **2015**, *482*, 55-61. DOI: 10.1016/j.ab.2015.04.021

8. Rovira-Llopis, S.; Rocha, M.; Falcon, R.; de Pablo, C. ; Alvarez A.; Jover A. ; Hernandez-Mijares, A. and. Victor, V. M., Is Myeloperoxidase a Key Component in the ROS-InducedVascular Damage Related to Nephropathyin Type 2 Diabetes ? *Antioxid. Redox. Sign.* **2013**, *19*, 1452-1458. DOI: 10.1089/ars.2013.5307
9. Galijasevic, S. The development of myeloperoxidase inhibitors. *Bioorg Med Chem Lett*. **2019,** *29*, 1-7. DOI: 10.1016/j.bmcl.2018.11.031
10. Jucaite, A.; Svenningsson, P.; Rinne, J. O.; Csele, Z.; Varna, K.; Johnström, P.; Amini, N.; Kirjavainen, A.; Helin, S.; Minkwitz, M.; Kugler, A. R.; Posener, J. A.; Budd, S.; Halldin, C.; Varrone, A. and Farde, L. Effect of the myeloperoxidase inhibitor AZD3241 on microglia: a PET study in Parkinson's disease. *Brain*. **2015**, *138*, 2687-2700. DOI: 10.1093/brain/awv184
11. Zhou, J.; Zhou, S. Inflammation: Therapeutic targets for diabetic neuropathies. *Mol. Neurobiol*. **2014,** *49*, 536-546. DOI: 10.1007/s12035-013-8537-0
12. Obrosova, I.G.; Ilnytska, O.; Lyzogubov, V.V.; Pavlov, I.A.;Mashtalir, N.; Nadler, J. L.; Drel, V.R. High-fat diet induced neuropathy of pre-diabetes and obesity: effects of "healthy" diet and aldose reductase inhibition. *Diabetes*. **2007**, *56*, 2598-2608. DOI: 10.2337/db06-1176 .
13. Sandireddy, R. Yerra, V.G., Areti, A. Komirishetty, P. and Kumar A. Neuroinflammation and oxidative stress in diabetic neuropathy: futuristic strategies based on these targets. *Int. J Endocrinol*. **2014**, *2014*, 674987. DOI: 10.1155/2014/674987
14. Pokhriyal, V., Kothiyal, P.; Kumar, N.; Kaushik, S. A review on diabetic neuropathy: Complications and treatment. *Asian J. Pharm. Pharmacol.* **2018**, *4*, 413-420. DOI: 10.31024/ajpp.2018.4.4.6
15. Hammes, H.P.; Du, X.; Edelstein, D.; Taguchi, T.; Matsumura, T.; Ju, Q.; Lin, J.; Bierhaus, A.; Nawroth, P.; Hannak, D.; Neumaier, M.; Bergfeld, R. Giardino, I.; Brownlee, M. Benfotiamine blocks three major pathways of hyperglycemic damage and prevents experimental diabetic retinopathy. *Nat. Med.* **2003**, *9*, 294–299. DOI: 10.1038/nm834
16. Varkonyi, T. and Kempler, P. Diabetic neuropathy: new strategies for treatment. *Diabetes Obes. Metab*., **2008**, *10*, 99-108. DOI: 10.1111/j.1463-1326.2007.00741.x
17. Tang, Y.; Chen, A. Curcumin eliminates the effect of advanced glycation end-products (AGEs) on the divergent regulation of gene expression of receptors of AGEs by interrupting leptin signaling. *Lab. Invest*. **2014**, *94*, 503–516. DOI: 10.1038/labinvest.2014.42
18. Khan, M.; Liu, H.; Wang, J. Sun, B. Inhibitory effect of phenolic compounds and plant extracts on the formation of advance glycation end products: A comprehensive review. *Food Res. Int.* **2020**, *130*, 108933. DOI: 10.1016/j.foodres.2019.108933
19. Shiba, Y.; Kinoshita, T.; Chuman, H.; Taketani, Y.; Takeda, E.; Kato, Y.; Naito, M.; Kawabata, K.; Ishisaka, A.; Terao, J.; Kawai, Y. Flavonoids as substrates and inhibitors of myeloperoxidase: molecular actions of aglycone and metabolites. *Chem Res Toxicol*. **2008**, *21*, 1600-1609. DOI: 10.1021/tx8000835
20. Galuppo, M.; Giacoppo, S.; Bramanti, P.; Mazzon, E. Use of natural compounds in the management of diabetic peripheral neuropathy. *Molecules*. **2014**, *19*, 2877-2895. DOI: 10.3390/molecules19032877
21. Singh, R.; Kaur, N.; Kishore, L.; Gupta, G. K. Management of diabetic complications: A chemical constituent based approach. *J. Ethno. Pharmacol*. **2013**, *150*, 51-70. DOI: 10.1016/j.jep.2013.08.051
22. Loke, W. M.; Proudfoot, J. M.; McKinley, A. J., Needs, P. W.; Kroon,P. A.; Hodgson,J. M.; Croft, K. D. Quercetin and its in vivo metabolites inhibit neutrophil-mediated low-density lipoprotein oxidation. *J Agric Food Chem.* **2008**, *56*, 3609-3615. DOI: 10.1021/jf8003042
23. Gargouri, B.; Carstensen, J.; Bathia, H. S.; Huell, M.; Dietz, G. P. H.; Fiebich, B. L. Anti-neuroinflammatory effects of Ginkgo Biloba extract EGb761 in LPS-activated primary microglial cells. *Phytomedicine* **2018**, *44*, 45-55. DOI: 10.1016/j.phymed.2018.04.009
24. Xie, B.; Wang, Q.; Zhou, C.; Wu, J.; Xu, D. Efficacy and Safety of the Injection of the Traditional Chinese Medicine Puerarin for the Treatment of Diabetic Peripheral Neuropathy: A Systematic Review and Meta-Analysis of 53 Randomized Controlled Trials. *Evid Based Complement Alternat Med.* **2018**, *2018*:2834650. DOI: 10.1155/2018/2834650
25. Liu, Q. S.; Pang, Z. R.; Liu, R.; He, G. R.; Cui, J. Yin, X.-Y. Effective compounds group of Mongolian prescriptions BAIMAI-SAN protect against peripheral neuropathy in lower limbs of rats through neuro protective effect. *J. Ethno. Pharmacol*. **2011**, *135*, 786-791. DOI: 10.1016/j.jep.2011.04.026

26. Hao, G. M. ; Liu Y. G.; Wu, Y.; Xing, W.; Guo, S.-Z.; Wang, Y.; Wang, Z.; Li, C.; Lv, T.-T.; Wang, H.-L.; Shi, T.-J. ; Wang, W.; Han, J. The protective effect of the active components of ERPC on diabetic peripheral neuropathy in rats. *J Ethnopharmacol*. **2017**, *202*, 162-171. DOI: 10.1016/j.jep.2017.03.015
27. Yang, X.; Yao, W. Li, Q.; Liu, H.; Shi, H.; Gao, Y.; Xu, L. Mechanism of Tang Luo Ning effect on attenuating of oxidative stress in sciatic nerve of STZ-induced diabetic rats. *J Ethnopharmacol*. **2015**, *174*, 1-10. DOI: 10.1016/j.jep.2015.07.047
28. Kandouli, C.; Cassien, M.; Mercier, A.; Ricquebourg, E.; Culcasi, M.; Stocker, P.; Mekaouche, M.; Leulmi, Z.; Mechakra, A.; Thétiot-Laurent, S.; Pietri S. Antioxidant and antidiabetic properties of water soluble extracts from *Anvillea radiata* in high-fat-fed mice. *J Ethnopharmacol;* **2017**, *207*, 251–267. DOI: 10.1016/j.jep.2017.06.042
29. Stocker, P.; Cassien, M.; Vidal, N.; Thétiot-Laurent, S. and Pietri, S. A fluorescent homogeneous assay for myeloperoxidase measurement in biological samples. A positive correlation between myeloperoxidase-generated HOCL level and oxidative status in STZ-diabetic rats. *Talanta* **2017**, *170*, 119-127. DOI: 10.1016/j.talanta.2017.03.102
30. Vidal, N.; Cavaille, J.P.; Graziani, F., Robin, M.; Ouari, O.; Pietri, S. and Stocker, P. High throughput assay for evaluation of reactive carbonyl scavenging capacity. *P. Redox Biol*. **2014**, *2*, 590-598. DOI: 10.1016/j.redox.2014.01.016
31. Ni, M.; Aschner, M. Neonatal rat primary microglia: isolation, culturing, and selected applications. *Curr Protoc Toxicol.* **2010**; Chapter 12: Unit 12.17.
32. Chu, J. M.; Lee, D. K.; Wong, D. P.; Wong, R. N.; Yung, K. K.; Cheng, C. H.; Yue, K. K. Ginsenosides attenuate methylglyoxal-induced impairment of insulin signaling and subsequent apoptosis in primary astrocytes. *Neuropharmacol*. **2014**, 85, 215-223. DOI: 10.1016/j.neuropharm.2014.05.029
33. De Gregorio, C.; Contador, D.; Campero, M.; Ezquer, M.; Ezquer, F. Characterization of diabetic neuropathy progression in a mouse model of type 2 diabetes mellitus. *Biol Open*. **2018**, *7*, bio036830. DOI: 10.1242/bio.036830
34. Cassien, M.; Petrocchi, C.; Thétiot-Laurent S.; Robin, M.; Ricquebourg, E.; Kandouli, C.; Asteian, A.; Rockenbauer, A.; Mercier, A.; Culcasi, M.; Pietri, S. On the vasoprotective mechanisms underlying novel β-phosphorylated nitrones: Focus on free radical characterization, scavenging and NO-donation in a biological model of oxidative stress. *Eur J Med Chem*. **2016**, *119*, 197-217. DOI: 10.1016/j.ejmech.2016.04.067
35. Chowdhury, S.; Ghosh, S.; Das, A. K.; Sil, P. C. Ferulic Acid Protects Hyperglycemia-Induced Kidney Damage by Regulating Oxidative Insult, Inflammation and Autophagy. *Front. Pharmacol.* **2019**, *10*, 27. DOI: 10.3389/fphar.2019.00027
36. Cos P; Ying L, Calomme, M.; Hu, J. P; Cimanga, K; Van Poel, B.; Pieters, L., Vlietinck, A. J. and Vanden Berghe, D. Structure-activity relationship and classification of flavonoids as inhibitors of xanthine oxidase and superoxide scavengers. *J Nat Prod*. **1998**; *61*, 71-76. DOI: 10.1021/np970237h
37. Lin, S.; Zhang, G.; Liao, Y.; Pan, J.; Gong, D. Dietary Flavonoids as Xanthine Oxidase Inhibitors: Structure-Affinity and Structure-Activity Relationships. *J Agric Food Chem*. **2015**; *63*, 7784-7794. DOI: 10.1021/acs.jafc.5b03386
38. Masuoka, N. and Kubo, I. Characterization of the xanthine oxidase inhibitory activity of alk(en)yl phenols and related compounds. *Phytochem*. **2018**, *155*, 100-106. DOI: 10.1016/j.phytochem.2018.07.006
39. Meotti, F. C.; Jameson, G. N.; Turner, R.; Harwood, D. T.; Stockwell, S.; Rees, M. D.; Thomas, S. R.; Kettle, A. J. Urate as a physiological substrate for myeloperoxidase: implications for hyperuricemia and inflammation. *J. Biol. Chem*. **2011**, *286*, 12901-12911. DOI: 10.1074/jbc.M110.172460
40. Neogi, T.; George, J.; Rekhraj, S.; Struthers, A. D.; Choi, H.; Terkeltaub, R. A. Are either or both hyperuricemia and xanthine oxidase directly toxic to the vasculature? A critical appraisal. *Arthritis Rheum*. **2012**, *64*, 327-338. DOI: 10.1002/art.33369
41. Mai X, Zhou F, Lin P, Gao, J.; Ma, Y.; Fan, R.; Ting, W.; Huang, C.; Yin, D.; Kang, Z. Metformin scavenges formaldehyde and attenuates formaldehyde-induced bovine serum albumin crosslinking and cellular DNA damage *Environ Toxicol.*, **2020,**1-9. DOI: 10.1002/tox.22982
42. Fakhruddin, S.; Alanazi, W. and Jackson K. E. Diabetes-Induced Reactive Oxygen Species: Mechanism of their generation and role in renal injury *J. Diabetes Res.*, **2017**, *2017*: 8379327. DOI: 10.1155/2017/8379327

43. Quattrini, L.; La Motta, C. Aldose reductase inhibitors: 2013-present. *Expert Opin Ther Pat*. **2019**, *29*, 199-213. DOI: 10.1080/13543776.2019.1582646
44. Obrosova, I. G. Increased sorbitol pathway activity generates oxidative stress in tissue sites for diabetic complications. *Antioxid Redox Signal*. **2005**, *7*, 1543-1552. DOI: 10.1089/ars.2005.7.1543
45. Flyvbjerg, A. Pathogenesis of microvascular complications in *Textbook of Diabetes*, Fifth Ed., Holt, R. I. G.; Cockram, C. S. and. Goldstein, B. J., Eds, 2017 JohnWiley & Sons, Ltd. DOI:10.1002/9781118924853.ch37
46. Galiniak, S; Bartosz, G.; Sadowska-Bartosz, I. Glutathione is the main endogenous inhibitor of protein glycation. *Gen Physiol Biophys*. **2017**, *36*, 175-186. DOI: 10.4149/gpb_2016044
47. Peng, X.; Ma, J.; Chen, F.; Wang, M. Naturally occurring inhibitors against the formation of advanced glycation end-products. *Food Funct*. **2011**; *2*, 289-301. DOI: 10.1039/C1FO10034C
48. O'Brien, P. D. ; Hinder, L. M.; Callaghan, B. C.; Feldman, L. E. Neurological consequences of obesity. *Lancet Neurol*. **2017**, *16*, 465-477. DOI: 10.1016/S1474-4422(17)30084-4
49. Klöting, N.; Blüher, M. Adipocyte dysfunction, inflammation and metabolic syndrome. *Rev. Endocr. Metab. Disord*. **2014**, *15*,277-287. DOI: 10.1007/s11154-014-9301-0
50. Terzo, S; Mulè, F; Caldara, G. F.; Baldassano, S.; Puleio, R.; Vitale, M.; Cassata, G.; Ferrantelli, V. and Amato, A. Pistachio Consumption Alleviates Inflammation and Improves Gut Microbiota Composition in Mice Fed a High-Fat Diet. *Int J Mol Sci*. **2020**, *21*, 365. DOI: 10.3390/ijms21010365
51. Xie, J.; Song, W.; Liang, X.; Zhang, Q.; Shi, Y.; Liu, W.; Shi, X. Protective effect of quercetin on streptozotocin-induced diabetic peripheral neuropathy rats through modulating gut microbiota and reactive oxygen species level. *Biomed Pharmacother*. **2020**, *127*, 110147. DOI: 10.1016/j.biopha.2020.110147
52. Spencer, J. P.; Vafeiadou, K.; Williams, R. J.; Vauzour, D. Neuroinflammation: modulation by flavonoids and mechanisms of action. *Mol Aspects Med*. **2012**, *33*, 83-97. DOI: 10.1016/j.mam.2011.10.016
53. Spagnuolo, C.; Moccia, S.; Russo, G. L. Anti-inflammatory effects of flavonoids in neurodegenerative disorders. *Eur J Med Chem*. **2018**, *153*, 105-115. DOI: 10.1016/j.ejmech.2017.09.001
54. Kim, M.; Choi, S. Y.; Lee, P.; Hur, J. Neochlorogenic Acid Inhibits Lipopolysaccharide-Induced Activation and Pro-inflammatory Responses in BV2 Microglial Cells. *Neurochem Res*. **2015**; *40*, 1792-1798. DOI: 10.1007/s11064-015-1659-1
55. Szwajgier, D; Borowiec, K.; Pustelniak, K. The neuroprotective effects of phenolic acids: Molecular mechanism of action. *Nutrients*. **2017**, *9*, 477. DOI: 10.3390/nu9050477
56. Shamsaldeen, Y. A., Mackenzie, L. S., Lione, L. A., Benham, C. D. Methylglyoxal, A Metabolite Increased in Diabetes is Associated with Insulin Resistance, Vascular Dysfunction and Neuropathies. *Curr. Drug. Metab.* **2016**. *17*, 359-67. DOI: 10.2174/1389200217666151222155216
57. Hansen, F.; Galland, F.; Lirio, F.; De Souza, D.; Ré, C.; Pacheco, R.; Vizuete, A.; Quincozes-Santos, A.; Leite, M.; Gonçalves, C.- A. Methylglyoxal Induces Changes in the Glyoxalase System and Impairs Glutamate Uptake Activity in Primary Astrocytes. *Oxid. Med. Cell. Longev*. **2017**, 2017: 9574201. DOI: 10.1155/2017/9574201
58. Belakredar, A.; Hachem, K.; Boudou, F. ; Benabdesslem, Y.; Megherbi, A. Acute Toxicity Study of Anvillea Radiata Aqueous Extract in Albino Rats. *J. Drug Deliv. Ther.* **2020**, *10*, 126-130. https://doi.org/10.22270/jddt.v10i5.4289
59. Uddin, M. S.; Mamun, A. A.; Rahman, M. A.; Kabir, M. T.; Alkahtani, S.; Alanazi, I. S.; Perveen, A.; Ashraf, G. M.; Bin-Jumah, M. N. and Abdel-Daim, M. M. Exploring the Promise of Flavonoids to Combat Neuropathic Pain: From Molecular Mechanisms to Therapeutic Implications. *Front. Neurosci.***2020**, *14*, 478. DOI: 10.3389/fnins.2020.00478
60. Basu, P.; Basu, A. In vitro and in vivo effects of flavonoids on peripheral neuropathic pain. *Molecules*. **2020**, 25, 1171. DOI: 10.3390/molecules25051171
61. Latha, R. C.; Daisy, P. Insulin-secretagogue, antihyperlipidemic and other protective effects of gallic acid isolated from Terminalia bellerica Roxb. in streptozotocin-induced diabetic rats. *Chem Biol Interact*. **2011**; *189*, 112-118. DOI: 10.1016/j.cbi.2010.11.005
62. Dhaliwal, J.; Dhaliwal, N.; Akhtar, A.; Kuhad, A.; Chopra, K. Beneficial effects of ferulic acid alone and in combination with insulin in streptozotocin induced diabetic neuropathy in Sprague Dawley rats. *Life Sciences*. **2020**, 255, 117856. DOI: 10.1016/j.lfs.2020.117856

63. Zhang, Y.-J, Lu, X. - W., Song, N.; Kou, L.; Wu, M.-K.; Liu, F.; Wang, H. and Shen, J.-F. Chlorogenic acid alters the voltage-gated potassium channel currents of trigeminal ganglion neurons. *Int J Oral Sci.* **2014**; *6*, 233-240. DOI: 10.1038/ijos.2014.58
64. Huang, S. M; Chuang, H. C; Wu, C. H.; Yen, G. C. Cytoprotective effects of phenolic acids on methylglyoxal-induced apoptosis in Neuro-2A cells. *Mol. Nutr. Food Res.* **2008**, 52, 940-949. DOI: 10.1002/mnfr.200700360
65. Hasanein, P; Mohammad Zaheri, L. Effects of rosmarinic acid on an experimental model of painful diabetic neuropathy in rats. *Pharm Biol*. **2014**, *52*, 1398-1402. DOI: 10.3109/13880209.2014.894090
66. Kosacka, J.; Woidt, K.; Toyka, K. V.; Paeschke, S.; Klöting, N.; Bechmann, I.; Blüher, M.; Thiery, J.; Ossmann, S.; Baum, P. and Nowicki, M. The role of dietary non-heme iron load and peripheral nerve inflammation in the development of peripheral neuropathy (PN) in obese non-diabetic leptin-deficient ob/ob mice. *Neurol Res*. **2019**, *41*; 341-353. DOI: 10.1080/01616412.2018.1564191
67. Yucel, Y.; Celepkolu, T.; Kibrisli, E.; Kilinc, F.; Beyaz, C.; Aluclu, M. U.; Basarili, M. K. and Ekinci, A.. Protective Effect of Caffeic Acid Phenethyl Ester on Oxidative Stress in Diabetic Rat Sciatic Nerve. *Int. J. Pharmacol,* **2012**, *8*, 577-581. DOI: 10.3923/ijp.2012.577.581
68. Nishat, S.; Klinke, A.; Balsdus, S. Khan, L. A. and Basir, S. F. Increased A_3AR-dependent vasoconstriction in diabetic mice is promoted by myeloperoxidase. *J. Cardiovasc. Pharmacol.* **2014**, *64*, 465-472. DOI: 10.1097/FJC.0000000000000139
69. Mizuno, Y.; Yamamotoya, T.; Nakatsu, Y.; Ueda, K.; Matsunaga, Y.; Inoue, M.-K.; Sakoda, H.; Fujishiro, M.; Ono, H.; Kikuchi, T.; Takahashi, M.; Morii , K.; Sasaki, K.; Masaki, T.; Asano, T. and Kushiyama A. Xanthine Oxidase Inhibitor Febuxostat Exerts an Anti-Inflammatory Action and Protects against Diabetic Nephropathy Development in KK-Ay Obese Diabetic Mice. *Int J Mol Sci*. **2019**, *20*, 4680. DOI: 10.3390/ijms20194680
70.